

First-principles investigations of ferroelectricity and piezoelectricity in BaTiO₃/PbTiO₃ superlattices

Yifeng Duan and Gang Tang

Department of Physics, China University of Mining and Technology, Xuzhou, Jiangsu Province 221116, People's Republic of China

Changqing Chen

Department of Engineering Mechanics, AML & CNMM, Tsinghua University, Beijing 100084, People's Republic of China

Tianjian Lu

School of Aerospace, Xi'an Jiaotong University, Xi'an, Shanxi Province 710049, People's Republic of China

Zhigang Wu*

Department of Physics, Colorado School of Mines, Golden, Colorado 80401, USA

(Received 25 June 2010; revised manuscript received 16 January 2012; published 13 February 2012)

The pressure dependence of ferroelectricity and piezoelectricity of a tetragonal BaTiO₃/PbTiO₃ (BPT) short-period superlattice is investigated using first-principles calculations. Our results suggest that, as the applied pressure increases, the BPT superlattice first becomes paraelectric at low pressures and then transfers to another ferroelectric phase at much higher pressures. Furthermore, a large enhancement of piezoelectricity close to the phase-transition regions is predicted, similar to that previously predicted in PbTiO₃. Comparing the BPT superlattice with bulk BaTiO₃ and PbTiO₃, we find that the BPT superlattice behaves very similarly to bulk BaTiO₃ under high pressures for the first transition, while it has much lower transition pressure and zero-pressure spontaneous polarization than those for PbTiO₃, although BPT has an equal number of BaTiO₃ and PbTiO₃ layers. However, for the second transition, BPT has a transition pressure close to the average of those for BaTiO₃ and PbTiO₃, and all three materials have similar pressure-induced polarization. Furthermore, our calculations indicate that the colossal enhancement in piezoelectricity is strongly correlated to phase transition when large atomic displacements can be generated by small external strain, but polarization rotation is not a necessary condition.

DOI: [10.1103/PhysRevB.85.054108](https://doi.org/10.1103/PhysRevB.85.054108)

PACS number(s): 77.65.-j, 77.84.-s, 77.80.-e

I. INTRODUCTION

Ferroelectric (FE) materials, which can convert mechanical energy to electrical energy and vice versa, have a wide range of applications in medical imaging, detectors, actuators, telecommunication, and ultrasonic devices. The crucial properties of these materials are ferroelectricity and piezoelectricity, which are sensitive to external conditions, such as strain, film thickness, temperature, external electric and magnetic fields, atomic substitution, chemical ordering, and pressure.¹ The most useful piezoelectric materials have a giant electromechanical response, discovered in relaxor-based complex solid solutions, such as PbMg_{1/3}Nb_{2/3}O₃-PbTiO₃ (PMN-PT) and PbZrO₃-PbTiO₃ (PZT), and previous theoretical investigations^{2,3} suggest that the noncollinear polarization rotation near the morphotropic phase boundary (MPB) is responsible for the giant piezoelectric response observed in these materials. Recent studies^{4,5} indicate that the polarization rotation and the MPB could even exist in pure perovskites, such as PT, under high pressures near phase-transition regions. Although under relatively low pressures ferroelectricity is suppressed and eventually a ferroelectric-to-paraelectric phase transition occurs,⁶ further increasing pressure leads to an anomalous paraelectric-to-ferroelectric phase transition, as demonstrated both theoretically and experimentally.⁷ The FE phase under very high pressures is distinct in nature from the conventional one at ambient conditions,^{7,8} in that the

new FE phase is electronically driven, rather than ionically driven in the latter. Moreover, our previous calculations drew similar conclusions about the variation of ferroelectricity in rhombohedral PT under uniaxial compression.⁹

Perovskite superlattices composed of alternating epitaxial ultrathin oxide layers are currently under intensive study due to their tunable and potentially excellent FE and piezoelectric properties. In these superlattices, strain due to lattice mismatch, charge compensation, their interface structures, and local asymmetries play important roles in enhancing spontaneous polarization.¹⁰⁻¹⁹ A recent publication by Cooper *et al.*²⁰ reported their theoretical studies on the effect of PT concentration on ferroelectricity and piezoelectricity of the BaTiO₃/PbTiO₃ (BPT) superlattice, consisting of the two most important simple perovskite ferroelectrics, BaTiO₃ (BT) and PbTiO₃, under in-plane compressive strain. They predicted an enhancement in the piezoelectric coefficient d_{33} , peaking at $\sim 75\%$ PT concentration with the minimum c/a axial ratio. Our previous computations^{21,22} indicate that the uniaxial tensile and in-plane compressive strains could greatly enhance piezoelectricity of BPT superlattices as well, in line with their results. However, no theoretical investigations have yet been done to study the effects of hydrostatic pressure on the FE and piezoelectric responses of the BPT superlattice.

In this work, we study the pressure effects on ferroelectricity and piezoelectricity of the tetragonal short-period BPT

superlattice, together with bulk BT and PT for comparison, using *ab initio* total-energy calculations as well as linear-response calculations. We find an anomalous paraelectric-to-ferroelectric phase transition under very high pressures and enormous enhancement in piezoelectricity near the phase-transition regions for the BPT superlattice, in good agreement with previous results for bulk BT and PT. The associated atomic displacements, Born effective charges, and electron-density distributions are also calculated to explain the origin of the predicted phenomena and quantify the effects of pressure.

II. COMPUTATIONAL METHODS

Our calculations are performed based on the density functional theory (DFT) within the local-density approximation (LDA), as implemented in the plane-wave pseudopotential ABINIT package.²³ A plane-wave energy cutoff of 40 hartrees and a $6 \times 6 \times 6$ \mathbf{k} -point mesh are used, ensuring good numerical convergence. The norm-conserving pseudopotentials generated by the OPIUM program have been tested against the all-electron full-potential linearized augmented plane-wave (LAPW) method.^{24,25} The orbitals of Ba $5s^25p^66s^2$, Pb $5d^{10}6s^26p^2$, Ti $3s^23p^63d^24s^2$, and O $2s^22p^4$ are explicitly included as valence electrons. To calculate the piezoelectric stress constants e_{iv} and elastic constants $c_{\mu\nu}$ (here Roman indexes run from 1 to 3, and Greek ones run from 1 to 6), we use the density functional perturbation theory (DFPT),^{26,27} which is based on the systematic expansion of the variational expression of the DFT total energy in powers of a variety of parameters, such as atomic coordinates, macroscopic strain, and electric field. Tensor e is the mixed second derivatives of total energy with respect to strain and electric field, while tensor c involves the second derivative of total energy with respect to strain. The piezoelectric strain coefficients $d_{iv} = \sum_{\mu=1}^6 e_{i\mu} s_{\mu\nu}$, where the elastic compliance tensor s is the reciprocal of elastic tensor c , and the electronic polarization \mathbf{P} is calculated using the well-known Berry-phase approach.^{28,29}

To find the equilibrium lattice constants under zero pressure, we optimize both the atomic positions and the lattice vectors of the primitive cell until the largest stress tensor components σ_{ij} are less than 0.05 GPa. Then we first apply a small compressive-strain increment η_3 along the c axis and conduct the full structural optimization until the following conditions are satisfied within a small tolerance of 0.05 GPa: $\sigma_{11} = \sigma_{22} = \sigma_{33} = -p$ and $\sigma_{ij} = 0$ for $i \neq j$, where p is the target pressure and η_3 is increased step by step to reach all the desired pressures. A similar approach has been taken to study the influence of uniaxial or biaxial strains on the mechanical, ferroelectric, and piezoelectric properties of tetragonal PT.^{31,32}

A double-perovskite ten-atom supercell along the z axis (c axis) is adopted for the short-period BPT superlattice, and the tetragonal $P4mm$ symmetry is kept for the crystal structures of BT, PT, and BPT. We choose the LDA instead of the widely used generalized gradient approximation (GGA) formulated by Perdew, Burke, and Ernzerhof³⁰ (PBE) since the PBE-GGA catastrophically overestimates both equilibrium volume and the strain for many prototype FE perovskites,³³ while the LDA only moderately underestimates these quantities. For tetragonal BT, our LDA results of lattice constants are

$a = 3.915 \text{ \AA}$ and $c = 3.995 \text{ \AA}$; for PT, they are $a = 3.843 \text{ \AA}$ and $c = 4.053 \text{ \AA}$, in good agreement with the experimental data of $a = 3.904 \text{ \AA}$ and $c = 4.152 \text{ \AA}$.³⁴ For the BPT superlattice, our calculated equilibrium lattice constants are $a = 3.897 \text{ \AA}$ and $c = 7.859 \text{ \AA}$.

III. RESULTS AND DISCUSSION

The top panels in Fig. 1 summarize the calculated pressure dependence of polarization. Under zero pressure, the calculated value of P for BPT is 0.29 C/m^2 , much less than 0.81 C/m^2 for PT and only slightly larger than the value of 0.28 C/m^2 for BT [the previous theoretical value is 0.26 C/m^2 (Ref. 20)]. This is because sharp interfaces in short-period ferroelectric superlattices strongly suppress the polarization, as suggested by Ref. 20; long-period BPT superlattices with the same PT concentration are expected to have a larger value of P than that in short-period ones.

As pressure increases, polarization in BT, PT, and BPT first decreases until reaching zero at critical pressures of about 10, 12, and 21 GPa, respectively, and this pressure-induced suppression of the FE instability and the consequent ferroelectric-to-paraelectric phase transition are well known and anticipated, consistent with previous experimental findings.^{35–37} Because the spontaneous polarization in BPT is very close to that in BT, its phase transition pressure is only 2 GPa higher; on the other hand, P in BPT is much lower than that in PT, leading to a 9-GPa decrease in transition pressure compared with PT.

As pressure further increases, the FE phase reappears at about 160, 58, and 113 GPa for BT, PT, and BPT, respectively, as summarized in Fig. 1. This anomalous paraelectric-to-ferroelectric phase transition has been predicted and experimentally verified previously,⁷ and the new FE phase under very high pressures is electronically driven, dramatically different in nature from the conventional ionically driven FE structure under ambient conditions, as discussed in detail in Ref. 7. Note that for the second phase transition, the transition pressure for BPT is almost the average of those for BT and PT, while it is very close to that for BT for the first transition. In addition, the increasing rates of P for BT, PT, and BPT with pressure become very close, as shown in the top panels of Fig. 1. These can be explained by the nature of electronically driven ferroelectricity under very high pressures, and in this state the atomistic details (e.g., Ba atoms compared with Pb atoms in BT and PT, respectively) do not strongly affect its ferroelectricity, in sharp contrast to the zero-pressure ionically driven FE state.

The tendencies of ferroelectricity are further emphasized in the bottom panels in Fig. 1 by the calculated lattice constant ratio c/a as a function of pressure. Similar to polarization, the values of c/a in these three materials first decrease rapidly with increasing pressure until reaching a constant for the paraelectric phase and remain unchanged in the broad range between the phase-transition pressures, and then they increase with the increasing pressure. For the zero-pressure structures, the c/a value of 1.055 for PT is much larger than that of 1.021 for BT, consistent with the fact that the spontaneous polarization of PT is much larger than that of BT. The c/a values of the paraelectric phase for both PT and BT are equal to 1.0, indicating a cubic crystal structure, whereas for

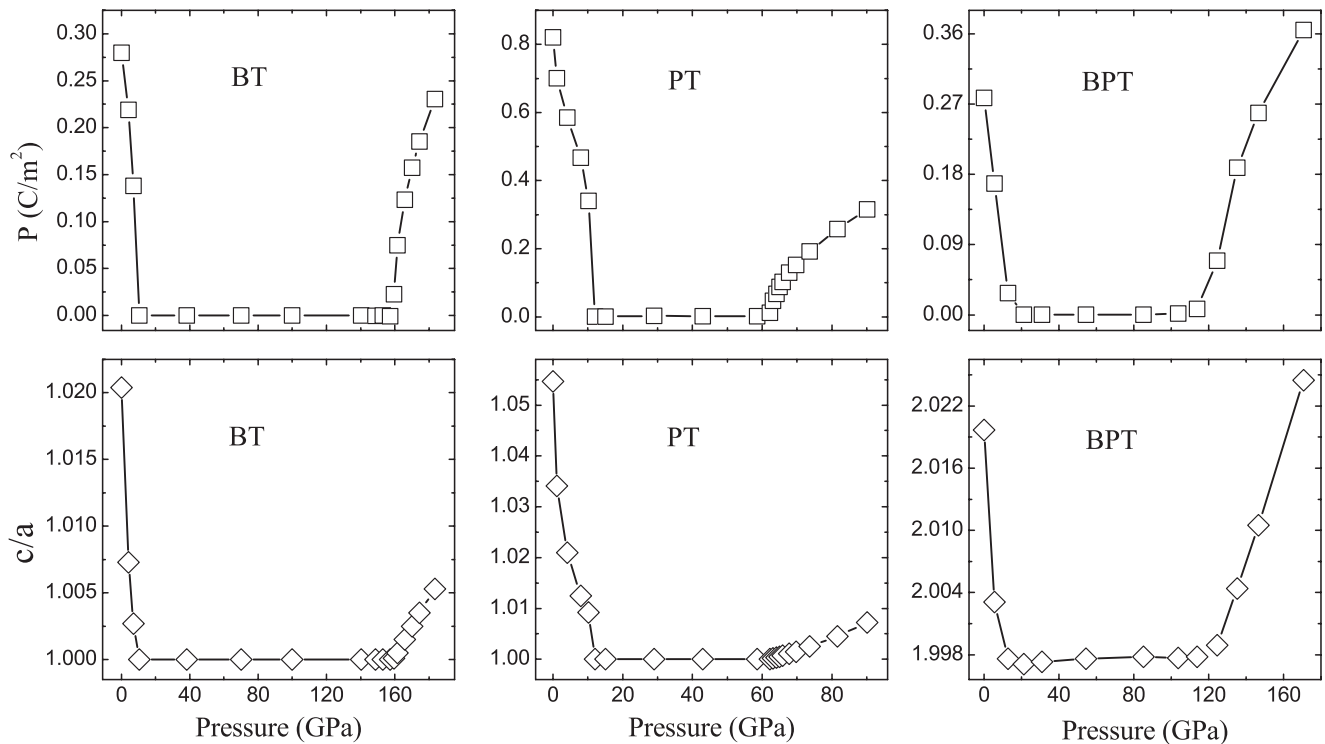


FIG. 1. Pressure dependence of polarization P (C/m²) and lattice constant ratio c/a for BaTiO₃ (BT), PbTiO₃ (PT), and the BaTiO₃/PbTiO₃ (BPT) superlattice.

the short-period BPT superlattice in the paraelectric pressure range, since the ionic radius of Ba²⁺ is shorter than that of Pb²⁺, its c/a value remains 1.997, slightly smaller than 2.0. When the second phase transition occurs, the increasing rate of c/a with respect to pressure for BT becomes very similar to that for PT, confirming that the high-pressure electronically driven ferroelectric phases in BT and PT behave very similarly, in contrast to the low-pressure ionically driven FE phase where the atomistic details dominate. The increasing rate of tetragonality with respect to pressure for BPT is very similar to that for PT or BT as well.

Figure 2 summarizes the pressure effect on piezoelectricity of BT, PT, and the BPT superlattice. Under zero pressure, the piezoelectric coefficients d_{31} and d_{33} (e_{31} and e_{33}) of BPT are between the corresponding values for BT and PT, e.g., the d_{33} value of 86 pC/N for BPT is smaller than 103 pC/N for PT, but larger than 36 pC/N for BT; on the other hand, d_{15} (e_{15}) of BPT is only half of that for BT and about 10% of that for PT. This is because d_{31} and d_{33} (e_{31} and e_{33}) describe the change of polarization along its direction due to normal strain (σ_{11} and σ_{33}), whereas d_{15} (e_{15}) corresponds to the change of \mathbf{P} perpendicular to its direction due to shear strain (σ_{13} and σ_{31}), and the displacements along the x axis for atoms in the BT layer are against those in the PT layer.

Our study concentrates on pressure effects on piezoelectric coefficients, which are greatly enhanced near phase transitions, e.g., the most significant enhancement is for d_{15} (e_{15}) of PT with the maximum value of 3750 pC/N (98 C/m²) near the ferroelectric-to-paraelectric phase transition (~ 10 GPa), in good agreement with the previously reported data.⁴ When a material approaches phase transition, its distinct phases with

different symmetries have very close free energies; thus the local energy minimum associated with each phase becomes shallow, and the potential well becomes very flat, resulting in large atomic displacements in response to external strain. All these piezoelectric coefficients for BT, PT, and BPT drop abruptly with further increasing pressure, and they remain zero in the paraelectric cubic (or pseudocubic) phase until the second phase transition occurs, where piezoelectricity is dramatically strengthened again, similar to the giant piezoelectricity enhancement at the first-phase-transition regions. An interesting observation is that d_{31} and d_{33} (e_{31} and e_{33}) all decrease rapidly after pressure passes the critical value for the second transition, while d_{15} (e_{15}) still increases slowly with increasing pressure.

In order to gain more understanding of the above observations, we plotted the atomic displacements μ and the Born effective charges Z^* as functions of pressure, as displayed in Fig. 3. Since the FE atomic displacements and the spontaneous polarization in a tetragonal structure are all along the c axis (z axis), only Z_{zz}^* contribute to \mathbf{P} . First of all, Z_{zz}^* for all these atoms barely change over the whole pressure range studied; among them, Z_{zz}^* of O₁ and O₄ atoms are very close to their nominal charges, whereas those of Ti, O₃, and O₆ atoms are anomalously large, suggesting the strong orbital hybridization between Ti₁ (and Ti₂) 3d and O₆ (and O₃) 2p states, as shown in the insets in Fig. 3. For the BPT superlattice, Z_{zz}^* of Ti₁ and Ti₂ atoms are very close to each other, which is also the case for O₁ and O₄ atoms, indicating that the values of Z_{zz}^* for Ti and O atoms are not sensitive to the different atomic environments (Pb²⁺ or Ba²⁺) in different layers. In contrast, the atomic displacements vary significantly with pressure,

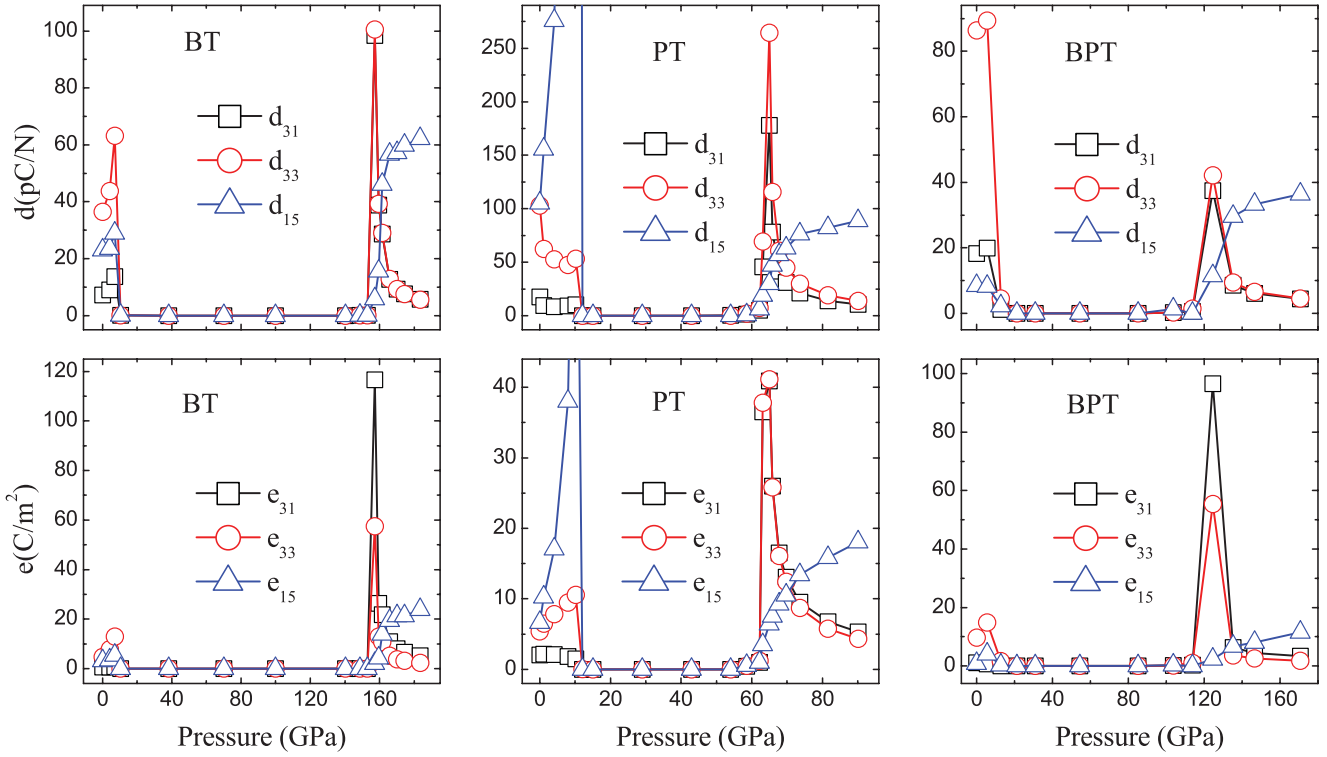


FIG. 2. (Color online) Pressure dependence of piezoelectric strain coefficients d_{31} , d_{33} , and d_{15} (pC/N) and piezoelectric stress coefficients e_{31} , e_{33} , and e_{15} (C/m^2) for BaTiO₃ (BT), PbTiO₃ (PT), and the BaTiO₃/PbTiO₃ (BPT) superlattice.

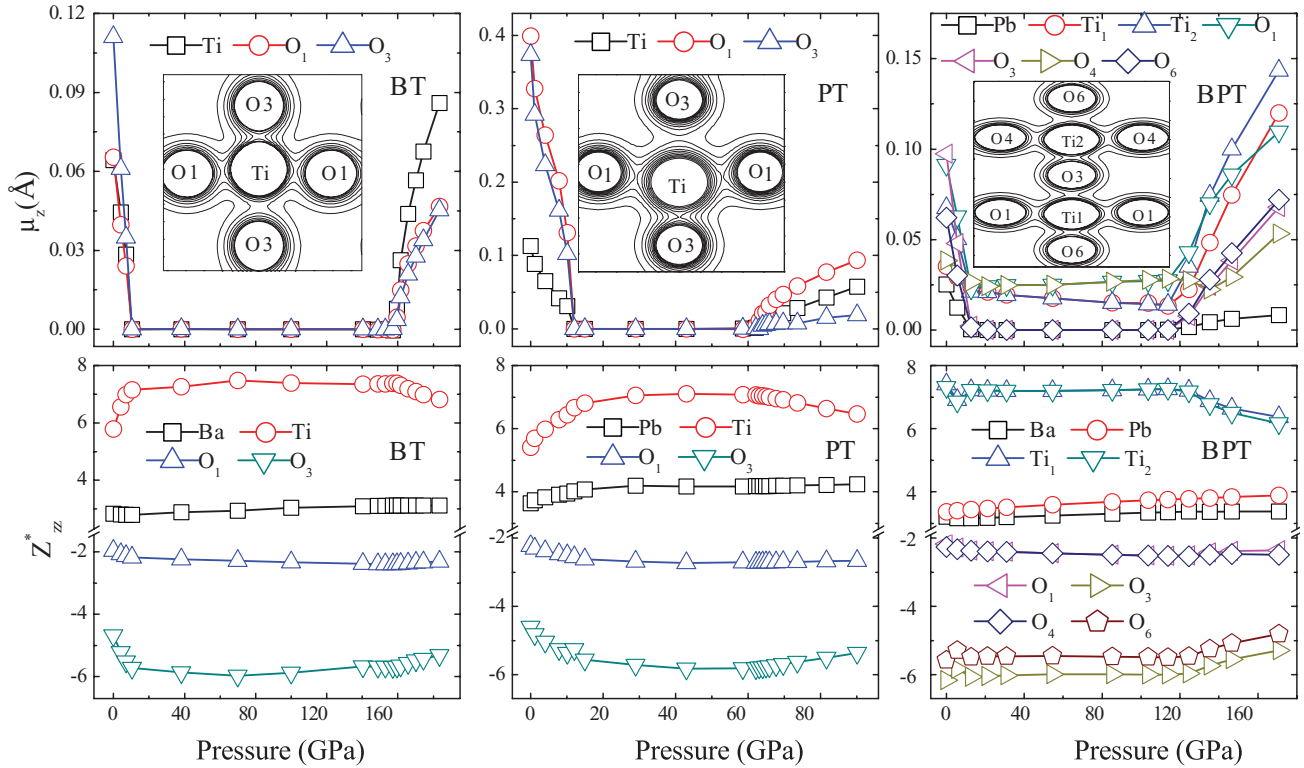


FIG. 3. (Color online) Pressure dependence of the atomic displacements μ along the c axis (in \AA) of the optimized structure relative to the centrosymmetric reference structure and the Born effective charges Z_{zz}^* for BaTiO₃ (BT), PbTiO₃ (PT), and the BaTiO₃/PbTiO₃ (BPT) superlattice. Note that the Ba atom in BT and BPT and the Pb atom in PT are fixed at the origin (0, 0, 0). The insets show the valence charge density along the c axis in the (200) plane under zero pressure, where the O₁ and O₄ (O₂ and O₅) atoms are on the xz (yz) face of the primitive cell and the O₃ and O₆ atoms are located between Ti atoms along the c axis.

particularly close to phase-transition regions. Therefore, the huge enhancement of piezoelectricity in these FE materials is due to large atomic displacements, instead of dramatic change of Born effective charges, when phase transitions occur.

In fact, Fig. 3 shows that atomic displacements as functions of pressure have nearly the same trends as the polarization and tetragonality ratio c/a , as compared with Fig. 1; as a result, the enhancement in piezoelectricity comes from almost purely crystal structural changes, rather than from electronic structure modification. Based on the above conclusion, the trends of individual piezoelectric coefficients illustrated in Fig. 2 can be easily understood from structural analysis. For instance, d_{31} and d_{33} (e_{31} and e_{33}) decrease rapidly after the second phase transition simply because the associated strains (σ_{11} and σ_{33}) do not change the polarization direction, and these quantities are just reduced to their normal values quickly above the phase-transition pressure. On the other hand, d_{15} (e_{15}) is caused by the shear strain (σ_{13} and σ_{31}), which changes (lowers) the $P4mm$ symmetry and causes polarization to rotate away from the c axis; therefore its value remains large even above the second transition pressure.

In Wu and Cohen's previous work,⁴ a complicated pressure-induced phase-transition sequence (tetragonal \rightarrow monoclinic \rightarrow rhombohedral \rightarrow cubic) is predicted by comparing the calculated enthalpy for a variety of different phases of PT under pressure. The monoclinic phase serves as an intermediate phase between the tetragonal and the rhombohedral phases, providing the required path for polarization rotation and resulting in the giant piezoelectric effects (e_{15} and d_{15} near the tetragonal-to-monoclinic transition and d_{33} near the monoclinic-to-rhombohedral transition). In this work, we constrain the symmetry to tetragonal $P4mm$ (which is a subgroup of cubic $Pm\bar{3}m$) so that the polarization always remains along the [001] direction, i.e., only the magnitude of polarization changes with pressure. Very similar trends for pressure-induced colossal enhancement in piezoelectricity are predicted when approaching the phase-transition regions; therefore, our current investigation suggests that polarization rotation is not a necessary condition for such huge enhancement in piezoelectricity; instead, it is the flat and shallow local energy minima associated with distinct phases that lead to such amazing phenomena.

It is well known that first-principles DFT calculations can only predict a material's properties at very low temperature, and a material's behaviors at low temperature might be different from those at room temperature. DFT calculations of ferroelectricity and piezoelectricity always assume 0 K; compared with room-temperature measurements, if the crystal structure is the same, the theoretical results of spontaneous polarization and piezoelectric coefficients are rather accurate.³⁸ In addition, the predicted reappearance of the FE phase of

PbTiO₃ under ultrahigh pressures was experimentally verified at room temperature;⁷ the huge enhancement of piezoelectricity under high pressures is due to phase transition, and thermal fluctuation may affect the phase-transition sequence and transition pressure but would not affect the appearance of the enhancement if phase transitions occur. In order to account for the effects of finite temperature on pressure-induced FE phase transitions, one can perform molecular dynamics (MD) or Monte Carlo (MC) simulations based on either the first-principles-derived effective Hamiltonian^{39,40,43} or a classical force field described by certain phenomenological models, such as the shell model with parameters fitted to DFT results.^{41,42} In addition, we have only computed the shortest-period BPT superlattice in this study, and similar calculations of BPT superlattices with arbitrary periodic thickness and composition are very demanding because of the large unit cells involved. A possible approach is to construct a model to describe the corresponding behaviors, with parameters fitted to DFT data for selected superlattices.

IV. SUMMARY

In summary, we have studied the pressure effects on ferroelectricity and piezoelectricity of tetragonal BT, PT, and their short-period BPT superlattice from first-principles computations. Anomalous phase transitions resulting in a second ferroelectric instability at very high pressures are predicted, accompanied by the giant enhancement of piezoelectricity occurring near the two phase-transition regions. The predicted huge electromechanical response originates from huge atomic displacements in response to strain near phase-transition regions because the effective Born charges do not change significantly with pressure. Our current calculations support the previous theory of the strong connection between phase transition and excellent piezoelectricity due to a very flat energy profile; however, polarization rotation is not required. This work sheds light on the origin of ultralarge piezoelectric response in complex relaxor-based ferroelectrics, and it should also stimulate more investigations on searching ferroelectric superlattices to make piezoelectric devices with better performance.

ACKNOWLEDGMENTS

The work is supported by the National Natural Science Foundation of China under Grants Nos. 11004242, 10947119, 10832002, and 11072127, the National Basic Research Program of China (Grant No. 2011CB610305), the Fundamental Research Funds for the Central Universities under Grant Nos. 2010LKWL01 and 2010LKWL02, the Youth Science Funds of China University of Mining and Technology under Grant No. 2009A040, and the start-up funds from Colorado School of Mines.

*zhiwu@mines.edu

¹M. E. Lines and A. M. Glass, *Principles and Applications of Ferroelectrics and Related Materials* (Clarendon, Oxford, 1979).

²H. Fu and R. E. Cohen, *Nature (London)* **403**, 281 (2000).

³Z. Wu and H. Krakauer, *Phys. Rev. B* **68**, 014112 (2003).

⁴Z. Wu and R. E. Cohen, *Phys. Rev. Lett.* **95**, 037601 (2005).

- ⁵M. Ahart, M. Somayazulu, P. Dera, H.-K. Mao, R. E. Cohen, R. J. Hemley, R. Yang, and Z. Wu, *Nature (London)* **451**, 545 (2008).
- ⁶J. A. Samnirjo, E. Lopez-Cruz, and G. Burns, *Phys. Rev. B* **28**, 7260 (1983).
- ⁷I. A. Kornev, L. Bellaiche, P. Bouvier, P.-E. Janolin, B. Dkhil, and J. Kreisel, *Phys. Rev. Lett.* **95**, 196804 (2005).
- ⁸E. Bousquet and P. Ghosez, *Phys. Rev. B* **74**, 180101 (2006).
- ⁹Y. Duan, J. Li, S.-S. Li, J.-B. Xia, and C. Chen, *J. Appl. Phys.* **103**, 083713 (2008).
- ¹⁰F. Le Marrec, R. Farhi, M. El Marssi, J. L. Dellis, M. G. Karkut, and D. Ariosa, *Phys. Rev. B* **61**, 6447 (2000).
- ¹¹J. B. Neaton and K. M. Rabe, *Appl. Phys. Lett.* **82**, 1586 (2003).
- ¹²J. Junquera and P. Ghosez, *Nature (London)* **422**, 506 (2003).
- ¹³C. H. Ahn, K. M. Rabe, and J.-M. Triscone, *Science* **303**, 488 (2004).
- ¹⁴H. N. Lee, H. M. Christen, M. F. Chisholm, C. M. Rouleau, and D. H. Lowndes, *Nature (London)* **433**, 395 (2005).
- ¹⁵S. M. Nakhmanson, K. M. Rabe, and D. Vanderbilt, *Appl. Phys. Lett.* **87**, 102906 (2005).
- ¹⁶M. Dawber, C. Lichtensteiger, M. Cantoni, M. Veithen, P. Ghosez, K. Johnston, K. M. Rabe, and J.-M. Triscone, *Phys. Rev. Lett.* **95**, 177601 (2005).
- ¹⁷D. D. Fong, A. M. Kolpak, J. A. Eastman, S. K. Streiffer, P. H. Fuoss, G. B. Stephenson, C. Thompson, D. M. Kim, K. J. Choi, C. B. Eom, I. Grinberg, and A. M. Rappe, *Phys. Rev. Lett.* **96**, 127601 (2006).
- ¹⁸E. Bousquet, M. Dawber, N. Stucki, C. Lichtensteiger, P. Hermet, S. Gariglio, J. M. Triscone, and P. Ghosez, *Nature (London)* **452**, 732 (2008).
- ¹⁹Z. Li, T. Lu, and W. Cao, *J. Appl. Phys.* **104**, 126106 (2008).
- ²⁰V. R. Cooper and K. M. Rabe, *Phys. Rev. B* **79**, 180101(R) (2009).
- ²¹Y. Duan, C. Wang, G. Tang, and C. Chen, *Nanoscale Res. Lett.* **5**, 448 (2010).
- ²²Y. Duan, L. Qin, G. Tang, and C. Chen, *Phys. Lett. A* **374**, 2075 (2010).
- ²³X. Gonze, J.-M. Beuken, R. Caracas, F. Detraux, M. Fuchs, G.-M. Rignanese, L. Sindic, M. Verstraete, G. Zerah, F. Jollet, M. Torrent, A. Roy, M. Mikami, Ph. Ghosez, J.-Y. Raty, and D. C. Allan, *Comput. Mater. Sci.* **25**, 478 (2002).
- ²⁴A. M. Rappe, K. M. Rabe, E. Kaxiras, and J. D. Joannopoulos, *Phys. Rev. B* **41**, 1227 (1990).
- ²⁵D. J. Singh, *Planewaves, Pseudopotential, and the LAPW Method* (Kluwer Academic, Boston, 1994).
- ²⁶S. Baroni, S. de Gironcoli, A. Dal Corso, and P. Giannozzi, *Rev. Mod. Phys.* **73**, 515 (2001).
- ²⁷D. R. Hamann, X. Wu, K. M. Rabe, and D. Vanderbilt, *Phys. Rev. B* **71**, 035117 (2005).
- ²⁸R. D. King-Smith and D. Vanderbilt, *Phys. Rev. B* **47**, 1651 (1993).
- ²⁹D. Vanderbilt and R. D. King-Smith, *Phys. Rev. B* **48**, 4442 (1993).
- ³⁰J. P. Perdew, K. Burke, and M. Ernzerhof, *Phys. Rev. Lett.* **77**, 3865 (1996).
- ³¹Y. Duan, H. Shi, and L. Qin, *J. Phys. Condens. Matter* **20**, 175210 (2008).
- ³²Y. Duan, L. Qin, G. Tang, and C. Chen, *J. Appl. Phys.* **105**, 033706 (2009).
- ³³Z. Wu, R. E. Cohen, and D. J. Singh, *Phys. Rev. B* **70**, 104112 (2004).
- ³⁴*Landolt-Börnstein: Zahlenwerte und Funktionen, 6th edition, Eigenschaften der Materie in ihren Aggregatzuständen, Part 8: Optische Konstanten*, edited by K. H. Hellwege and A. M. Hellwege (Springer-Verlag, Berlin, 1962), Vol. 2.
- ³⁵G. A. Samara, T. Sakudo, and K. Yoshimitsu, *Phys. Rev. Lett.* **35**, 1767 (1975).
- ³⁶J. A. Sanjurjo, E. Lopez-Cruz, and G. Burns, *Phys. Rev. B* **28**, 7260 (1983).
- ³⁷A. Sani, B. Noheda, I. A. Kornev, L. Bellaiche, P. Bouvier, and J. Kreisel, *Phys. Rev. B* **69**, 020105 (2004).
- ³⁸G. Sághi-Szabó, R. E. Cohen, and H. Krakauer, *Phys. Rev. Lett.* **80**, 4321 (1998).
- ³⁹W. Zhong, D. Vanderbilt, and K. M. Rabe, *Phys. Rev. Lett.* **73**, 1861 (1994).
- ⁴⁰W. Zhong, D. Vanderbilt, and K. M. Rabe, *Phys. Rev. B* **52**, 6301 (1995).
- ⁴¹M. Sepliarsky and R. E. Cohen, *AIP Conf. Proc.* **626**, 36 (2002).
- ⁴²T. Shimada, K. Wakahara, Y. Umeno, and T. Kitamura, *J. Phys. Condens. Matter* **20**, 325225 (2008).
- ⁴³G. Geneste, *Phys. Rev. B* **79**, 064101 (2009).